



# A kinetic analysis for production of calcium borogluconate from colemanite

Fatih Demir | Anas Osamah Ali Al-Ani | Omer Lacin

Chemical Engineering Department,  
Engineering Faculty, Ataturk University,  
Erzurum, Turkey

## Correspondence

Fatih Demir, Chemical Engineering  
Department, Engineering Faculty, Ataturk  
University, Erzurum, Turkey.  
Email: fatihdemir@atauni.edu.tr

## Abstract

In this paper, the kinetic model of colemanite dissolution in gluconic acid solutions was carried out in a batch reactor. The effects of the particle size, reaction temperature, stirring speed, gluconic acid concentration, and solid/liquid ratio on colemanite dissolution were experimentally studied. The empirical parameters were the gluconic acid concentration (0.05–0.2 M), the temperature (20–50°C), the solid/liquid ratio (0.05/500–1.5/500 g·L<sup>-1</sup>), particle size (193.5–1000 μm), and stirring speed (400–700 rpm).

The kinetic models for heterogeneous solid-liquid reactions were used with the dissolution data in evaluating the kinetic. The dissolution of colemanite in gluconic acid solutions was controlled by diffusion through the product layer. The activation energy was found to be 8.39 kJ·mol<sup>-1</sup>. The rate expression associated with the dissolution rate of colemanite depending on the parameters chosen may be summarized as follows:

$$1 - 3(1 - X)^{2/3} + 2(1 - X) = 1.2 e^{-8.39/RT_t}$$

## KEYWORDS

colemanite, dissolution kinetics, gluconic acid, solid-liquid reaction, calcium borogluconate

## 1 | INTRODUCTION

Turkey has more than two third of the world boron reserves in the form of ulexite, colemanite, and tinkal.<sup>1–3</sup> Boron attracts attention among the most essential elements in the

world because of its critical value in the industry. It is found in the form of metal borates, but boron is never found in free form in nature. In nature, more than 230 kinds of boron minerals can be found. Economically usable minerals of boron are hydrate compounds of calcium, sodium, and magnesium elements. Recently, boron and its compounds have found extensive use in the industry. It is frequently used in medicine, nuclear engineering, agricultural catalysts, fuel for rocket motors, ceramics, in steels, polymers, and glass-paint industries.<sup>4,5</sup>

Colemanite is one of the most important compounds of boron in the industry. The chemical formula of colemanite is 2CaO·3B<sub>2</sub>O<sub>3</sub>·5H<sub>2</sub>O.<sup>6,7</sup> Colemanite ore has a monoclinic crystal structure containing hydrated calcium borate and many clay minerals. The favorite boron mineral in the industry is colemanite used in boric acid production,

**Nomenclature:** aq, aqueous solution; C, concentration of gluconic acid solution, mol·L<sup>-1</sup>; C<sub>A</sub>, concentration of A in the bulk solution, mol·L<sup>-1</sup>; D, mean particle size (m) arithmetical average of upper and lower sieve sizes; D<sub>e</sub>, diffusion coefficient, m<sup>2</sup>·s<sup>-1</sup>; E, activation energy, kJ·mol<sup>-1</sup>; K, reaction rate constant, s<sup>-1</sup>; K<sub>d</sub>, mass transfer coefficient, m·s<sup>-1</sup>; k<sub>0</sub>, preexponential factor, s<sup>-1</sup>; k<sub>s</sub>, rate constant for surface reaction, mol·s<sup>-1</sup>; L, amount of liquid, L; r, regression coefficient; R, universal gas constant, 8.314 J mol<sup>-1</sup> K<sup>-1</sup>; R<sub>s</sub>, average radius of solid particle sphere, m; s, solid; t, reaction time, min; T, temperature, K; t\*, time for complete conversion, min; X, fraction of B converted, the conversion, X<sub>B</sub> = X; ρ<sub>B</sub>, molar density of solid reactant, mol·L<sup>-1</sup>

**TABLE 1** The studies on the dissolution kinetics of colemanite ore with organic and inorganic acids

Borate mineral	Acid	Researcher and date	Reference
	Acetic acid	Ozmetin et al (1996)	20
	Oxalic acid	Bayca et al (2014)	21
	Citric acid	Cavus and Kuslu (2005)	22
Colemanite	Phosphoric acid	Temur et al (2000)	23
	Ammonium nitrate	Gur (2008)	24
	Sulfuric acid	Sis et al (2019)	25

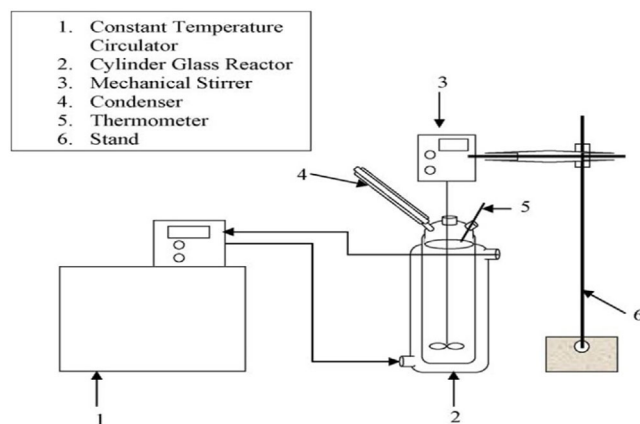
manufacture of heat-resistant glass and cleaning operators.<sup>8,9</sup> It is generally used to produce boric acid. However, a large class of boron chemicals utilizes the boric acid as a starting material in the preparation of organic boron salts and boron esters, which are the most often utilized boron compounds.<sup>10-13</sup>

Gluconates and gluconic acid have a great influence on the production industries of detergent, food, pharmaceutical, feed, and many other industries.<sup>14,15</sup> The production of gluconates and gluconic acid salts can be generated by biochemical, electrochemical, and other chemical methods.<sup>16,17</sup> In recent years, calcium, magnesium, and sodium gluconate produced by fermentation have been studied by many researchers.<sup>18,19</sup>

There are many studies related to the colemanite dissolution kinetics in alternative organic and inorganic solutions. Some of these studies are given in Table 1.

In addition to boric acid, calcium borogluconate is produced as a by-product from the reaction of gluconic acid and colemanite. It is particularly used in the feed industry and contains many vitamins for plants and animals. Calcium borogluconate is used in the hypocalcemia treatment of sheep, cattle, and goats. It is called parturient paresis and commonly known milk fever. Milk fever is one of the most common problems during the period just before and after parturition, in which a decrease in the amount of calcium in the blood occurs. Low calcium content in the blood creates many bone diseases after parturition. Therefore, calcium supplements are applied to cattle, sheep, etc. for treatment of milk fever. It consists of injecting the calcium borogluconate to the vein to provide calcium ions and to keep the plasma calcium concentration at a sufficient level. This process is very important to protect animal health.<sup>26,27</sup>

The aim of this study is to investigate dissolution kinetics of the colemanite ore in gluconic acid solutions to contribute to the calcium borogluconate production. The kinetics of the reaction between colemanite ore and gluconic acid were statistically studied by using heterogeneous and homogeneous reaction models. The most appropriate equation for experimental data was determined. The process parameters are the temperature of reaction, the speed of stirring, gluconic acid concentration, solid/liquid

**FIGURE 1** The experimental set up a schematic diagram [Color figure can be viewed at wileyonlinelibrary.com]**TABLE 2** The chemical analysis of colemanite mineral

Component (wt %)							
B <sub>2</sub> O <sub>3</sub>	CaO	H <sub>2</sub> O	SiO <sub>2</sub>	Al <sub>2</sub> O <sub>3</sub>	MgO	Fe <sub>2</sub> O <sub>3</sub>	Others
44.20	26.75	22.20	3.19	0.92	1.41	0.43	0.90

ratio, and particle size of colemanite. This investigation presents an elective solution for the assessment of the production of mineral colemanite ore.

## 2 | MATERIALS AND METHODS

### 2.1 | Materials

The colemanite mineral, which was used in the experiment, was obtained from Kutahya, Turkey. The process of dissolution was performed in a jacketed glass reactor of 750 mL volume supported by a mechanical stirrer as shown in Figure 1. Additionally, the glass reactor was fitted with a condenser to prevent vapor loss. The samples were crushed and then ground and then sieved to size fractions 193.5, 277, 668.5, and 1000  $\mu\text{m}$  using ASTM standard sieves. The chemical analyses of the mineral and B<sub>2</sub>O<sub>3</sub> amount in various colemanite particles are illustrated by Tables 2 and 3. The pH of solutions was adjusted by adding a few drops 0.1 M HCl or 0.1 M NaOH solution and monitored

**TABLE 3** The amount of B<sub>2</sub>O<sub>3</sub> in various colemanite particle sizes

Size of Particle (μm)	1000	668.5	277	193.5
B <sub>2</sub> O <sub>3</sub> (%)	47	44	45.8	46.7

by a digital pH-meter (model Thermo Orion 3 Star pH-meter). Analytical-grade HCl, NaOH, and mannitol were purchased from Merck, and distilled water was used in the experiments. Gluconic acid (50% by weight solution in water), an organic acid, was used in all experiments.

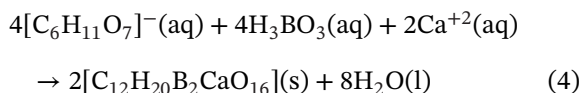
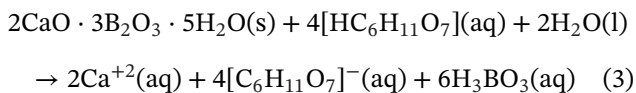
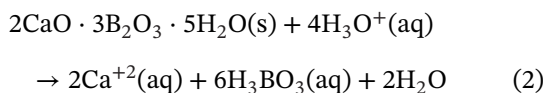
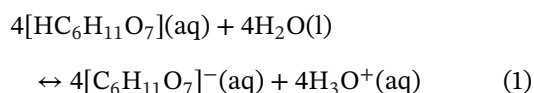
## 2.2 | Experimental procedure

Before starting the experiments, 500 mL of gluconic acid solution was put into the glass reactor. The solution was heated until the solution temperature reached the desired constant temperature. Then, 1 g of solid colemanite was added to the solutions while stirring the contents of the reactor at a determined speed. At certain time intervals, 1 mL samples of the reacted solution were quickly taken from the reactor at determined times and filtered. After this process, the volumetrical method was used to analyze B<sub>2</sub>O<sub>3</sub> amount in the filtrated sample.<sup>28</sup> The degree of dissolution of colemanite was determined as a function of time.

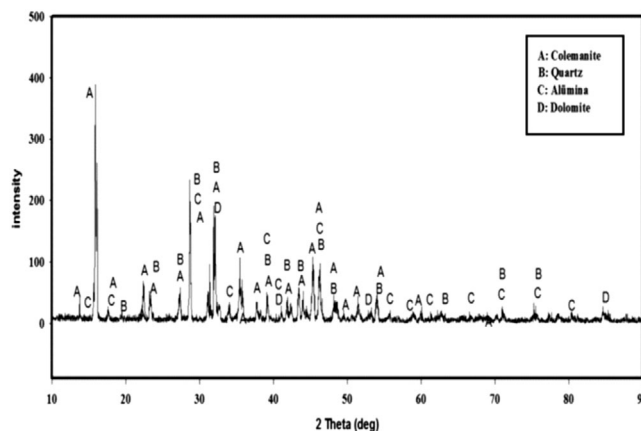
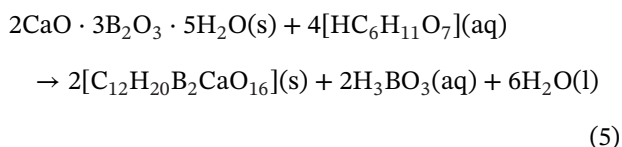
## 3 | RESULTS AND DISCUSSION

### 3.1 | Dissolution reactions

Reactions between colemanite and gluconic acid can be written as Equations (1-5)



and the final reaction:

**FIGURE 2** XRD of colemanite ore used in experiments**TABLE 4** The chosen parameters for dissolution of colemanite in gluconic acid solutions and their values

Parameters	Values
Particle size (μm)	1000, 688.5, <u>277</u> , 193.5
Acid concentration (M)	0.05, <u>0.1</u> , 0.15, 0.2
Solid/liquid ratio (g·mL <sup>-1</sup> )	0.5/500, 0.75/500, <u>1/500</u> , 1.5/500
Stirring speed (rpm)	400, <u>500</u> , 600, 700
Temperature (°C)	20, <u>30</u> , 40, 50

### 3.2 | XRD diffractogram of colemanite

A Bruker-AXS D8 Advance model XRD instrument, coupled with monochromatic Cu K $\alpha$  radiation ( $\lambda = 0.1542 \text{ \AA}$ ), was used to examine the mineralogical composition of the colemanite and operated at a scan rate of  $0.02^\circ \text{ min}^{-1}$  for  $2\theta$  between  $10^\circ$  and  $90^\circ$ . The characteristic peaks, in which the main component is colemanite, can be seen in a XRD diffractogram of colemanite shown in Figure 2.

### 3.3 | The effects of parameters

The effects of process factors such as the gluconic acid concentration, the solution temperature, colemanite particle size, solid/liquid ratio, and stirring speed on the dissolution rate of colemanite were examined. The chosen parameters for dissolution of colemanite in gluconic acid solutions and their values can be seen in Table 4. Table 4 also shows that the parameters that were kept constant at values that are underlined, while the impact of other parameters in the experiments was examined. The stirring speed was kept constant in all the experiments at 500 rpm to maintain the homogeneity of suspension in the reactor. The data obtained from experiments were plotted in the form of time versus fractional conversion as shown in

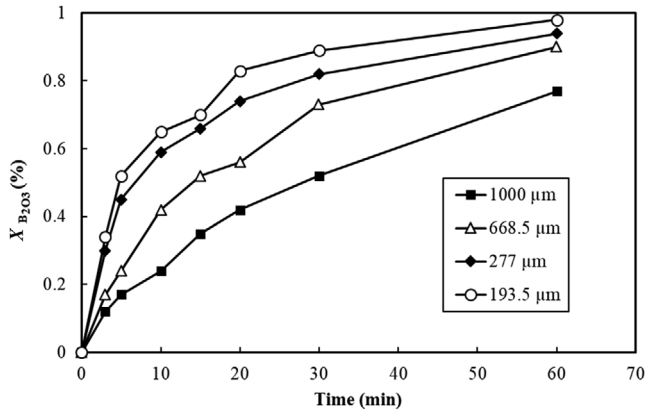


FIGURE 3 Effect of particle size on colemanite dissolution

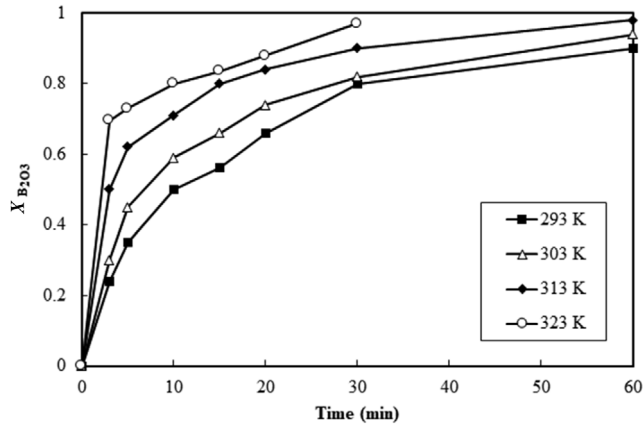


FIGURE 4 Effect of temperature on colemanite dissolution

Figures 3–7. The conversion fraction  $X$  (%) was calculated from Equation (6):

$$X_{B_2O_3} (\%) = \frac{B_2O_3 \text{ amount in the solution (g)}}{B_2O_3 \text{ amount in the original sample (g)}} \times 100. \quad (6)$$

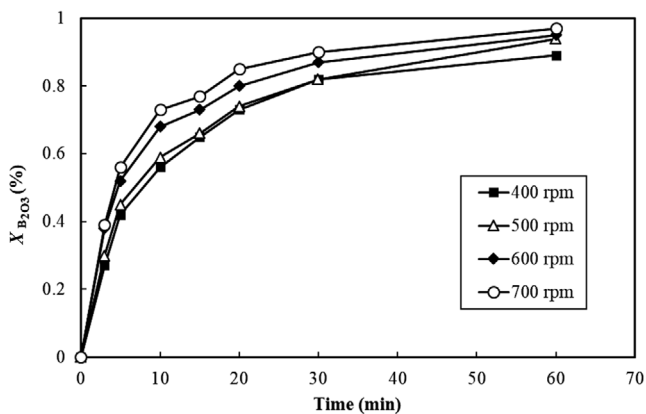


FIGURE 5 Effect of stirring speed on the dissolution of colemanite

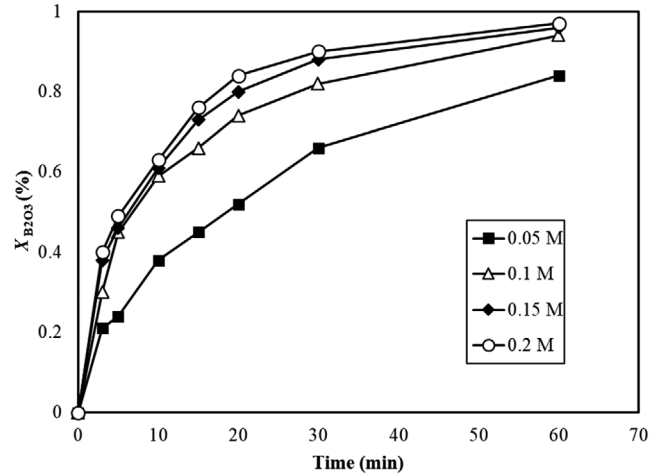


FIGURE 6 Effect of acid concentration on the dissolution of colemanite

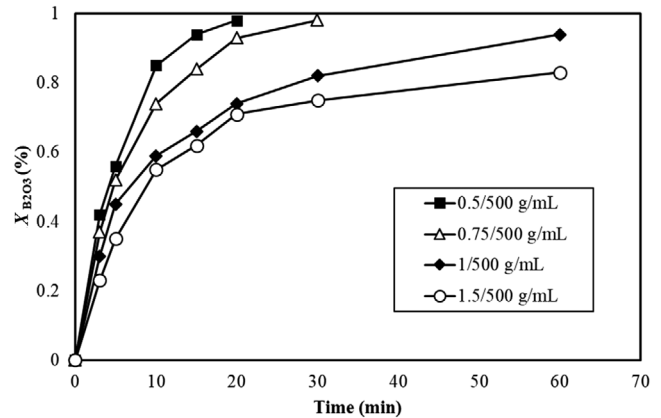


FIGURE 7 Effect of the solid/liquid ratio on the dissolution of colemanite

### 3.4 | Effect of particle size

Particle size effects on the dissolution rate were investigated for different particle sizes of 193.5, 277, 668.5, and 1000  $\mu\text{m}$ . Other parameters were kept constant including the following: temperature is 30°C, solid/liquid ratio is 1/500  $\text{g}\cdot\text{mL}^{-1}$ , stirring speed is 500 rpm, and gluconic acid concentration is 0.1 M. As seen in Figure 3, the dissolution rate increases as the particle size decreases. This result is due to the increase in surface area of the samples as the particle size decreases.

### 3.5 | Effect of reaction temperature

The dissolution experiments were performed at the temperature of 20, 30, 40, and 50°C, while the other parameters were kept constant at 0.1 M gluconic acid

concentration, 1/500 g·mL<sup>-1</sup> solid/liquid ratio, stirring speed of 500 rpm, and 227 μm particle size. The obtained results from experimental data are shown in Figure 4. As seen in Figure 4, the dissolution rate increases as the temperature increases. The dissolution rate at high temperature was 97%.

### 3.6 | Effect of stirring speed

To determine the effect of the stirring speed on the dissolution rate of colemanite, effect of stirring speed was investigated at 400, 500, 600, and 700 rpm. The change between stirring speed and conversion rate can be seen in Figure 5. It can be seen from Figure 5 that there is no effect of stirring speed on the dissolution rate of colemanite when the other parameters were kept constant at 227 μm, 1 M, 1/500 g·mL<sup>-1</sup>, and 30°C. Similar results have been reported in the literature for dissolution of colemanite.<sup>20,22,29</sup> Homogeneous suspension was obtained at a stirring speed of 500 rpm. Therefore, the stirring speed rate of 500 rpm was chosen as the constant value in all experiments.

### 3.7 | Effects of acid concentration

The effects of colemanite dissolution in gluconic acid in different concentrations were studied. The experiments were carried out with different gluconic acid concentrations of 0.05, 0.1, 0.15, and 0.2 M where other parameters were fixed at 227 μm, 500 rpm, 1/500 g·mL<sup>-1</sup>, and 60°C. The experimental data is plotted in Figure 6. The results showed that the increase in acid concentration causes an increase in the rate of colemanite dissolution.

### 3.8 | Effect of solid/liquid ratio

The effect of the solid/liquid ratio on colemanite dissolution rate was studied for 0.5/500, 0.75/500, 1/500, and 1.5/500 g·mL<sup>-1</sup>, while other parameters were kept constant at 227 μm, 500 rpm, 0.1 M, and 30°C, as shown in Figure 7. According to Figure 7, the decrease in the solid/liquid ratio leads to an increase in the dissolution rate. This result can be attributed to the decrease in the number of colemanite particles per amount of solutions.

### 3.9 | Kinetic analysis

Solid-fluid reactions are abundant and have considerable industrial significance. The solid-fluid reaction rate can be

obtained from the heterogeneous and homogeneous reaction models. In the homogeneous reaction model, the liquid reactant enters the surface of the particle and reacts at all times throughout the particle. Thus, the solid reactive behave as if it were dissolved.<sup>29</sup> In the heterogeneous model, the reaction is considered to take place at the outer surface of the unreacted particle. With the increase in conversion, the unreacted core of the particle shrinks and the layer of the solid product thickens. The kinetics of a noncatalytic reaction between solid and fluid can be studied utilizing the unreacted shrinking core model. One of the three ideal stages can represent the process rate controlled by diffusion through fluid film control, diffusion through product film control, and chemical reaction control.<sup>30</sup> Here, the model that determines the reaction rate is the model that depends on the highest resistance. To determine the rate of the control step, the empirical data were analyzed. The kinetic equations were also examined to determine the rate of B<sub>2</sub>O<sub>3</sub> passing into solution considering the effects of the parameters. Multiple regression analysis in the Statistica Package 8.0 program, and graphical method were applied to determine which step controls the present system in terms of the unreacted core and the other models. The integrated rate equations and the correlation coefficients for these models are given in Table 5.

Table 5 shows that the best *r*<sup>2</sup> values and experimental data correlate well with equation, which means that the dissolution rate is controlled by the diffusion through the product layer. As colemanite particles are nonporous, the most appropriate reaction model appears to be that of shrinking nonporous particles. Since the stirring speed is not impacted by the dissolution rate, it is deduced that the diffusion through the fluid film does not act as a rate-controlling step.

The integrated rate equation for diffusion through product film for spherical solids with diameter *D* is given by Equation (7):

$$1 - 3(1 - X)^{2/3} + 2(1 - X) = kt. \quad (7)$$

In this model, the fractional conversion, *X*, is given as a function of the reaction time. The variation of  $[1 - 3(1 - X)^{2/3} + 2(1 - X)]$  with time is plotted for colemanite particle sizes and reaction temperatures in Figures 8 and 9, respectively. It can be seen from these figures that the straight lines for all samples have correlation coefficients between 0.9575 and 0.9951.

When the reaction is product layer diffusion controlled, *R<sub>s</sub>*<sup>2</sup> and *t*<sup>\*</sup> values must be linearly dependent. If the *t*<sup>\*</sup> values are plotted versus *R<sub>s</sub>*<sup>2</sup>, the obtained curve is a straight line and this verifies that the reaction is product layer diffusion controlled (Figure 10).

TABLE 5 Integrated rate equations for the unreacted core and the other models, and regression analyses

Rate controlling	Step rate equation	$r^2$
Film diffusion	$\frac{t}{t^*} = X_B t^* = \frac{\rho_B^R}{3bk_s C_A}$	0.8309
Diffusion through product	$\frac{t}{t^*} = 1 - 3(1 - X_B)^{2/3} + 2(1 - X_B) \quad t^* = \frac{\rho_B^R}{6bD_p C_A}$	0.9696
Chemical reaction	$\frac{t}{t^*} = 1 - (1 - X_B)^{1/3} \quad t^* = \frac{\rho_B^R}{bk_s C_A}$	0.9468
Film diffusion (large grain)	$kt = 1 - (1 - X)^{1/2} \quad t^* = \frac{\rho_B^R}{bk_s C_A}$	0.9245
Film diffusion (small grain)	$kt = 1 - (1 - X)^{2/3} \quad t^* = \frac{\rho_B^R}{bk_s C_A}$	0.8966
First-order pseudohomogeneous model	$kt = -\ln(1 - X)$	0.9653
Second-order pseudohomogeneous model	$kt = X/(1 - X)$	0.8959

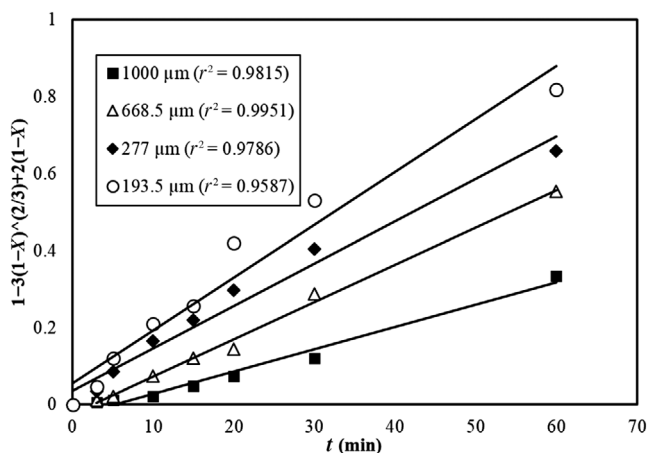


FIGURE 8 Variation of the model time for different particle sizes

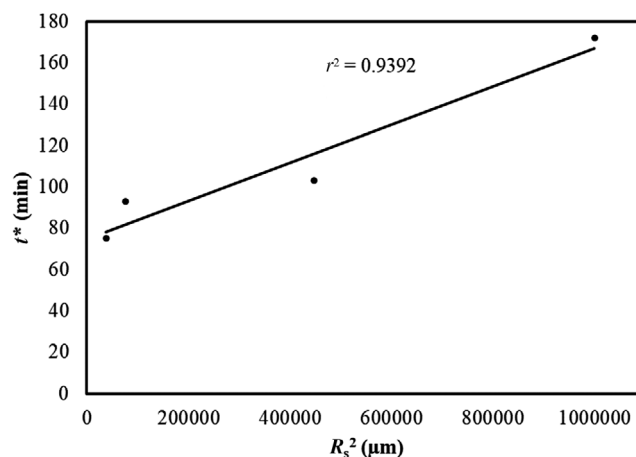
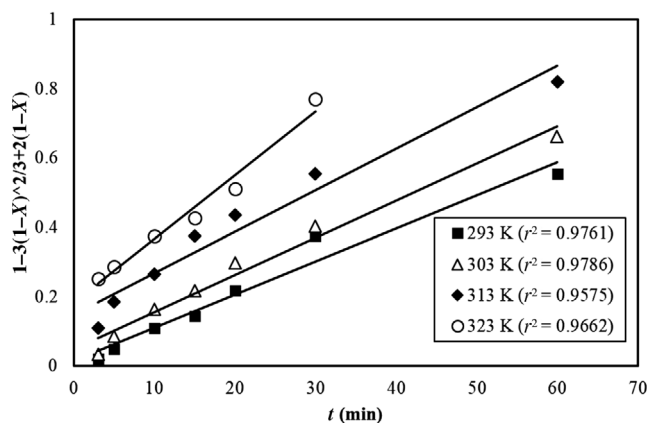
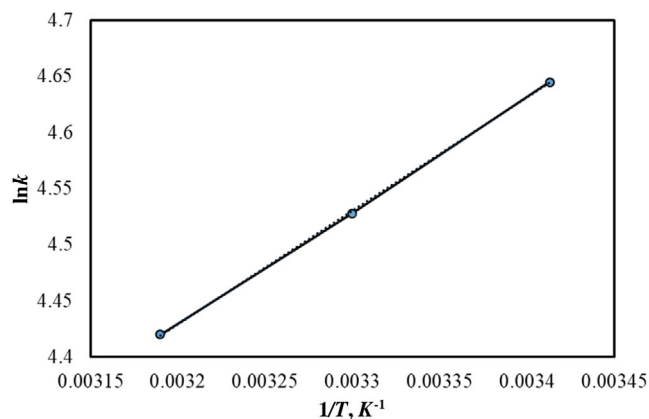
FIGURE 10 Agreement between  $t^*$  and  $R_s^2$ 

FIGURE 9 Variation of the model with time for different temperatures

The rate constants ( $k$ ) obtained from the slopes of Figure 9 are used in the Arrhenius equation (8):

$$k = k_0 e^{-E/RT}, \quad (8)$$

$$\ln k = \ln k_0 - \frac{E}{RT}. \quad (9)$$

FIGURE 11  $\ln k$  versus  $1/T$  [Color figure can be viewed at [wileyonlinelibrary.com](http://wileyonlinelibrary.com)]

According to Equation (9), a plot of  $\ln k$  versus  $1/T$  should be a straight line with a slope  $-E/R$  and intercept  $\ln k_0$  (Figure 11). The  $B_2O_3$  apparent activation energy and preexponential factor from Figure 11 were calculated as  $8.39 \text{ kJ}\cdot\text{mol}^{-1}$  and  $1.2 \text{ s}^{-1}$  respectively.

The activation energy of processes controlled with diffusion is characterized to be from  $4.18$  to  $12.55 \text{ kJ}\cdot\text{mol}^{-1}$ , while

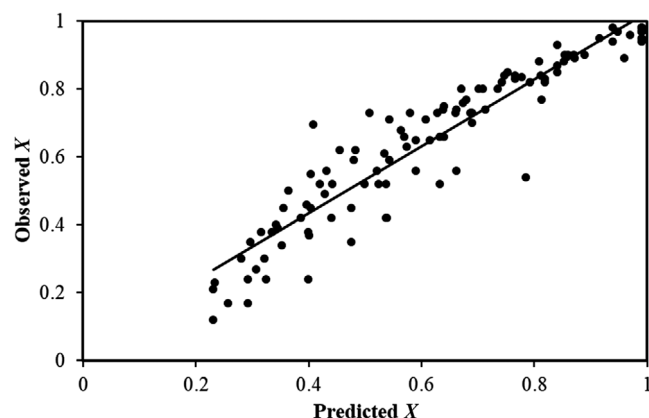


FIGURE 12 Agreement between observed values and predicted values from the model

for a chemically controlled process it is usually greater than  $41.84 \text{ kJ}\cdot\text{mol}^{-1}$ .<sup>31</sup>

Since the activation energy is low, it can be said that the diffusion from the product layer was controlling the dissolution rate of colemanite in gluconic acid solutions. Similar results were found by Alkan and Dogan,<sup>29</sup> Guliyev et al,<sup>8</sup> and Karagoz and Kuslu.<sup>22</sup> They found that the dissolution rate of colemanite was controlled by diffusion through the product layer, and the activation energies are 39.71, 26.34, and 28.65  $\text{kJ}\cdot\text{mol}^{-1}$ , respectively.

When  $k$  and  $E$  are plugged into Equation (9), the following kinetic model (Equation 10) is obtained:

$$1 - 3(1 - X)^{2/3} + 2(1 - X) = 1.2 e^{-8.39/RT} t. \quad (10)$$

The comparison between the observed values and predicted values obtained from this model can be seen in Figure 12. The values obtained from the model were found to be in good agreement with the observed values.

## 4 | CONCLUSION

In this study, the dissolution of colemanite in gluconic acid solutions was investigated. Five parameters such as acid concentration, reaction temperature, solid/liquid ratio, particle size, and stirring speed were investigated. It was found that the increase in the acid concentration and the reaction temperature increased the dissolution rate, the decrease in particle size, and solid/liquid ratio caused an increase in the dissolution rate. Based on the result of the examination, the impact of stirring speed on the rate of the dissolution of colemanite in gluconic acid was found to have no effect, which explains that the diffusion through the fluid film does not act as a rate-controlling step. It was found that the rate-controlling step

was controlled by a shrinking core model with the heterogeneous diffusion controlled through the ash or product layer. The apparent activation energy of the reaction was found as  $8.39 \text{ kJ}\cdot\text{mol}^{-1}$ . Thus, it can be said that calcium borogluconate is produced with this kinetic model.

## ORCID

Fatih Demir  <https://orcid.org/0000-0003-0264-1074>

## REFERENCES

1. Simsek HM, Guliyev R, Bese AV. Dissolution kinetics of borogypsum in di-ammonium hydrogen phosphate solutions. *Int J Hydrogen Energy*. 2018;43(44):20262-20270.
2. Cetin E, Eroglu I, Ozkar S. Kinetics of gypsum formation and growth during the dissolution of colemanite in sulfuric acid. *J Cryst Growth*. 2001;231(4):559-567.
3. Sis H, Bentli I, Demirkiran N, Ekmekyapar A. Dissolution kinetics of colemanite in HCl solutions by measuring particle size distributions. *Sep Sci Technol*. 2018;53(1):198-205.
4. Sahinkaya HU, Ozkan A. Investigation of shear flocculation behaviors of colemanite with some anionic surfactants and inorganic salts. *Sep Purif Technol*. 2011;80(1):131-139.
5. Tunc M, Kocakerim MM, Kucuk O, Aluz M. Dissolution of colemanite in  $(\text{NH}_4)_2\text{SO}_4$  solutions. *Korean J Chem Eng*. 2007;4(1):55-59.
6. Demirkiran N. A study on dissolution of ulexite in ammonium acetate solutions. *Chem Eng J*. 2008;141(1-3):180-186.
7. Karagoz O, Kuslu S. Dissolution kinetics of colemanite in potassium dihydrogen phosphate solution ( $\text{KH}_2\text{PO}_4$ ). *Int J Hydrogen Energy*. 2017;42(36):23250-23259.
8. Guliyev R, Kuslu S, Calban T, Colak S. Leaching kinetics of colemanite in potassium hydrogen sulphate solutions. *J Ind Eng Chem*. 2012;18(1):38-44.
9. Kizilca M, Copur M. Kinetic investigation of reaction between colemanite ore and methanol. *Chem Eng Commun*. 2015;202:1528-1534.
10. Kavci E, Calban T, Colak S, Kuslu S. Leaching kinetics of ulexite in sodium hydrogen sulphate solutions. *J Ind Eng Chem*. 2014;20(5):2625-2631.
11. Piskin MB. Investigation of sodium borohydride production process: "wexite mineral as a boron source". *Int J Hydrogen Energy*. 2009;34(11):4773-4779.
12. Ekmekyapar A, Demirkiran N, Kunkul A. Dissolution kinetics of ulexite in acetic acid solutions. *Chem Eng Res Des*. 2008;86(9a):1011-1016.
13. Taylan N, Gurbuz H, Bulutcu AN. Effects of ultrasound on the reaction step of boric acid production process from colemanite. *Ultrason Sonochem*. 2007;4(5):633-638.
14. Bayrak B, Lacin O, Bakan F, Sarac H. Investigation of dissolution kinetics of natural magnesite in gluconic acid solutions. *Chem Eng J*. 2006;117(2):109-115.
15. Pal P, Kumar R, Banerjee S. Manufacture of gluconic acid: a review towards process intensification for green production. *Chem Eng Process*. 2016;104:160-171.
16. Ramachandran S, Fontanille P, Pandey A, Larroche C. Gluconic acid: properties, applications and microbial production. *Food Technol Biotech*. 2006;44(2):185-195.

17. Rao DS, Panda T. Comparative-analysis of calcium gluconate and sodium gluconate techniques for the production of gluconic acid by *Aspergillus niger*. *Bioprocess Eng.* 1993;8(5-6):203-207.
18. Bao J, Furumoto K, Fukunaga K, Nakao K. A kinetic study on air oxidation of glucose catalyzed by immobilized glucose oxidase for production of calcium gluconate. *Biochem Eng J.* 2001;8(2):91-102.
19. Vavrusova M, Skibsted LH. Spontaneous supersaturation of calcium D-gluconate during isothermal dissolution of calcium L-lactate in aqueous sodium D-gluconate. *Food Funct.* 2014;5(1):85-91.
20. Ozmetin C, Kocakerim MM, Yapici S, Yartasi A. A semiempirical kinetic model for dissolution of colemanite in aqueous CH<sub>3</sub>COOH solutions. *Ind Eng Chem Res.* 1996;35(7):2355-2359.
21. Bayca SU, Kocan F, Abali Y. Dissolution of colemanite process waste in oxalic acid solutions. *Environ Prog Sustain.* 2014;33(4):1111-1116.
22. Cavus F, Kuslu S. Dissolution kinetics of colemanite in citric acid solutions assisted by mechanical agitation and microwaves. *Ind Eng Chem Res.* 2005;44(22):8164-8170.
23. Temur H, Yartasi A, Copur M, Kocakerim MM. The kinetics of dissolution of colemanite in H<sub>3</sub>PO<sub>4</sub> solutions. *Ind Eng Chem Res.* 2000;39(11):4114-4119.
24. Gur A. A kinetic study on leaching of colemanite in ammonium nitrate solutions. *Chinese J Inorg Chem.* 2008;24(3):467-473.
25. Sis H, Bentli I, Demirkiran N, Ekmekyapar A. Investigating dissolution of colemanite in sulfuric acid solutions by particle size measurements. *Sep Sci Technol.* 2019;54(8):1353-1362.
26. Seifi HA, Mohri M, Zadeh JK. Use of pre-partum urine pH to predict the risk of milk fever in dairy cows. *Vet J.* 2004;167(3):281-285.
27. Chamberlin WG, Middleton JR, Spain JN, Johnson GC, Ellersieck MR, Pithua P. Subclinical hypocalcemia, plasma biochemical parameters, lipid metabolism, postpartum disease, and fertility in postparturient dairy cows. *J Dairy Sci.* 2013;96(11):7001-7013.
28. Gulensoy H. *Kompleksometrik Titrasyonlar ve Kompleksometrinin Temelleri.* Istanbul, Turkey: Fatih Yayınevi; 1974.
29. Alkan M, Dogan M. Dissolution kinetics of colemanite in oxalic acid solutions. *Chem Eng Process.* 2004;43(7):867-872.
30. Levenspiel O. *Chemical Reaction Engineering, 3rd edn.* New York, NY: Wiley; 1999.
31. Abdel-Aal EA. Kinetics of sulfuric acid leaching of low-grade zinc silicate ore. *Hydrometallurgy.* 2000;55:247.

**How to cite this article:** Demir F, Al-Ani AOA, Lacin O. A kinetic analysis for production of calcium borogluconate from colemanite. *Int J Chem Kinet.* 2020;52:769–776.  
<https://doi.org/10.1002/kin.21398>